1-1-2013

The Effect of αCT-1 Peptide on Bone Marrow Stromal Cells Following Injury

Adam Clay Vandergriff
University of South Carolina

The effect of αCT-1 peptide on bone marrow stromal cells following injury

by

Adam Vandergriff

Bachelor of Engineering
Vanderbilt University 2011

Submitted in Partial Fulfillment of the Requirements

for the Degree of Master of Science in

Biomedical Engineering

College of Engineering and Computing

University of South Carolina

2013

Accepted by:

Dr. Jay Potts, Director of Thesis

Dr. John Eberth, Commitee Member

Dr. Lacy Ford, Vice Provost and Dean of Graduate Studies

Acknowledgments

I would like to thank my advisor, Dr. Jay Potts, for his guidance throughout all of my research, Dr. John Eberth for being on my thesis committee, Dr. Bob Price and the staff of the IRF for help with confocal microscopy, Dr. John Fuseler for help with live cell imaging, Charity Dunn for help with western blotting, Lorain Junor for her help and advice, and my lab-mates Dr. Keith Moore, Chad Simmons, and Brian Bennett for their help and support.

Abstract

Connexin43 (Cx43) is a component of gap junctions and is involved in intercellular signaling following injury to tissues. The carboxyl terminus of Cx43 binds to the PDZ2 domain of ZO-1 in order to form gap junction plaques and connect to the cytoskeleton. A biomimetic peptide known as αCT-1, replicating the last 9 amino acids found in the carboxyl terminus of CX43, has been shown to improve wound healing by preferentially binding to the PDZ2 domain of ZO-1. A possible mechanism for its action is through the Epithelial-Mesenchymal Transformation (EMT). Scratch assays were performed on rat bone marrow stromal cells treated with the peptide and were then analyzed using qPCR, western blotting, confocal microscopy, and live cell imaging. The gene expression analysis showed up-regulation of F11r and Krt19 and down-regulation of Mmp3. Protein expression analysis indicated an increase in Krt19 and the complete absence of Snai2 in the αCT-1 treated samples. Confocal microscopy suggested increased actin remodeling, increased size of Cx43 gap junctions, and reduction and localization of Mmp3 to the nucleus. Live cell imaging showed an increase in migration for the first seven hours followed by a breakdown in cell to cell contact. The genes and proteins chosen in this study did not indicate the changes of EMT; however, migration and morphology of the cells were similar to that of cells undergoing EMT. This study provides a beginning look into the mechanism of αCT-1 and will aid in its future development as a treatment for enhancing healing capabilities.

Table of Contents

List of Tables

List of Figures

Chapter 1

Introduction

Wound healing is a process that requires numerous signaling mechanisms to coordinate actions between multiple cells. One mechanism for the spread of signals related to a wound is through protein structures known as gap junctions. Some signals are beneficial to wound healing, yet the spread of apoptotic signals through gap junctions can increase tissue damage (Lin et al. 1998). The natural mechanism to prevent tissue damage through gap junction signaling, is to close and reduce gap junctions (Peters et al. 1993). In particular, it has been shown that down-regulation of Connexin43 (Cx43) at a wound site reduces inflammation and improves migration and proliferation (Mori et al. 2006). In tissues dependent upon gap junctions for healthy functions such as the heart and brain, this loss of signaling can lead to further damage. Biomimetic peptides such as αCT-1 have been shown to limit tissue damage and improve healing after injury, yet the exact mechanism of action has not been determined.

1.1 Gap Junctions

Gap junctions are one of many membrane proteins found in cells. Gap junctions create channels between the cytoplasm of adjacent cells that allow for the passage of molecules less than 1 kDa in size (Alexander and Goldberg 2003). They are critical to tissue function in the heart, neurons, and smooth muscle. Gap junctions are made of subunit proteins called connexins. Cx43 is one of the most commonly expressed connexin proteins, existing in many different tissues throughout the body (Beyer,

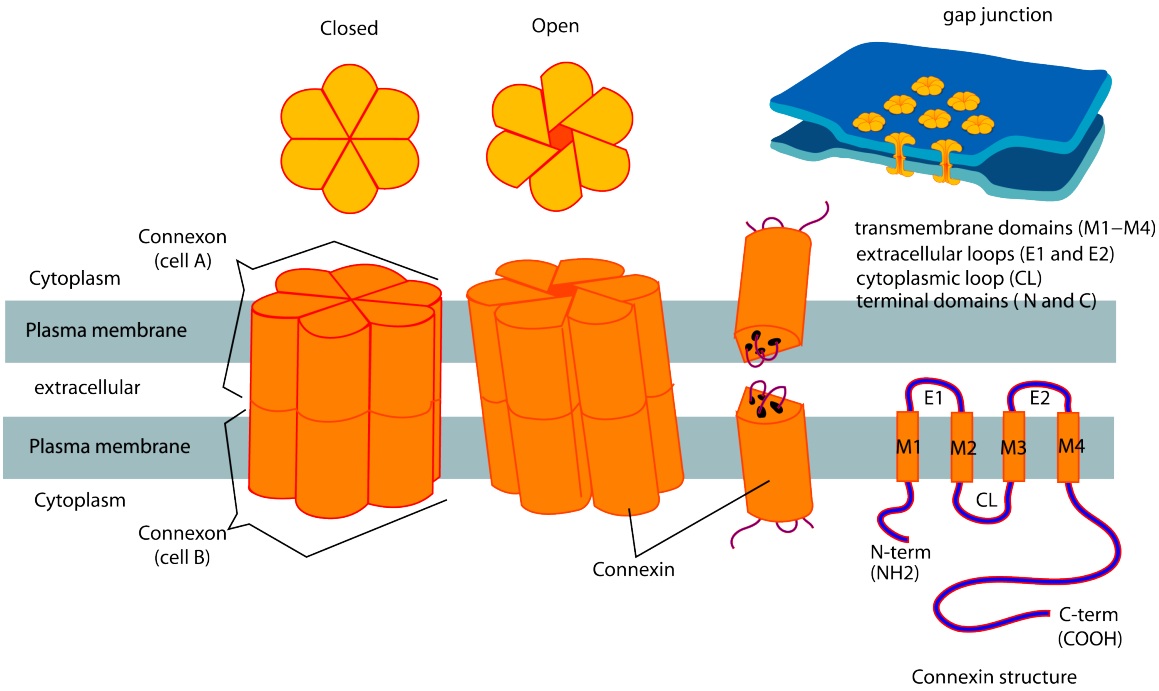

Figure 1.1: General structure of connexins, connexons, and gap junction plaques (Ruiz 2006).

Paul, and Goodenough 1987; Solan and Lampe 2009). It is essential for normal heart function as it allows for the transmission of action potentials, and in a mouse model its deletion resulted in death (Reaume et al. 1995). It consist of four transmembrane regions (M1-M4), two extracellular loops (EL1-EL2), a cytoplasmic loop (CL), a short amino terminus (NT), and a long carboxyl terminus (Cx43CT) (Milks et al. 1988; Kumar and Gilula 1996). Connexins combine to form hexameric connexons which then combine to create gap junctions, but there are numerous regulatory steps that control the formation and coupling of gap junctions.

The entire process of assembly and transportation is intricate and regulated by numerous signals (for review see Segretain and Falk 2004). Briefly, the connexins are transcribed in the endoplasmic reticulum (ER) then assembled into connexons upon leaving the ER (Musil and Goodenough 1993). These can be composed of one type of connexin or multiple types (He et al. 1999). After transport through the Golgi Apparatus, the connexons are transported in vesicles along microtubules, then

integrated into the cell membrane. In the membrane, connexons can exist as either hemichannels or gap junctions. Hemichannels allow molecules to flow in and out of the cell through the pore. Hemichannels can also align at 30 degree offsets (Perkins, Goodenough, and Sosinsky 1998) and dock with others in adjacent cells to create gap junctions through which small molecules can flow between cells (Friend and Gilula 1972; Unger et al. 1999; Goodenough and Paul 2009). These gap junctions typically form aggregates known as plaques.

In order for Cx43 connexons to leave the Golgi apparatus and migrate to the membrane, they must be transported by a membrane-associated guanylate kinase (MAGUK) protein known as Zonula Occludens-1 (ZO-1) (Wu, Tsai, and Chung 2003). ZO-1 escorts the Cx43 connexon to the edge of the plaque, and then inserts it into the plaque where it will couple to form a gap junction (Rhett, Jourdan, and Gourdie 2011). This region surrounding plaques with a high concentration of ZO-1 bound hemichannels is known as the perinexus (Palatinus, Rhett, and Gourdie 2012). ZO-1 is also known to disassemble the plaques, and shRNA silencing of ZO-1 results in a lack of plaque disassembly and increased intracellular Cx43 due to inability to be transported to the membrane (Akoyev and Takemoto 2007). The carboxyl terminus of Cx43 (Cx43CT) interacts with the PDZ2 domain of ZO-1 (Toyofuku et al. 1998; Giepmans and Moolenaar 1998) which alters the function of Cx43 as well as serving as a scaffold to connect Cx43 to the cytoskeleton and other proteins (Fanning, Ma, and Anderson 2002).

1.2 Connexin43 Carboxyl Terminus

The Cx43CT is the most studied region of the protein as it contains numerous regulation sites which can be modified or bind to various proteins (Giepmans 2004). It is capable of dimerizing with other Cx43CTs (Sorgen et al. 2004a), binding to the cytoplasmic loop to block the pore due to changes in pH (Duffy et al. 2002) and

voltage (Moreno 2002) and even binding to nearby cytoplasmic loops (Stergiopoulos et al. 1999). Other proteins shown to bind to the Cx43CT include Akt (Park et al. 2009), CCN3 (Fu et al. 2004), v-Src (Lin et al. 2001), c-Src (Sorgen et al. 2004b), and P2Y1 (Scemes 2008).

The carboxyl terminus of Cx43 consists of 150 residues, starting at the end of the M4 region around residue 230 and culminating at residue 382 as shown in Figure 1.2. In these 150 residues there are 21 serine residues and 1 tyrosine residue that can be phosphorylated. The effect of phosphorylation on the Cx43CT is still being investigated, but it has been shown that the Cx43CT typically exists in at least three different states of phosphorylation: P0, P1, and P2. Upon initial translation, Cx43 is in the P0 state with no phosphorylation. Upon reaching the membrane it is typically changed to the P1 (Ser365) then the P2 (Ser325, Ser328, Ser330) state and becomes a functional gap junction (Solan and Lampe 2009).

In particular there are several phosphorylation sites crucial to the functioning of Cx43 gap junctions during injury. Under ischemic conditions in the heart, Cx43 uncouples and migrates away from intercalated disks. Phoshporylation at Ser368 by protein kinase C (PKC) has been shown to reduce Cx43 gap junction conductivity (Ek-Vitorin et al. 2006; Bao, Reuss, and Altenberg 2004) and increase Cx43 gap junctions disassembly by ZO-1 (Akoyev and Takemoto 2007). This phosphorylation can be prevented by phosphorylation at Ser365 which is normally phosphorylated in healthy tissue (Solan et al. 2007).

1.3 αCT-1 Peptide

Recent research has focused on the use of biomimetic peptides that interfere with the function of Connexin43 due to its roles in tissue damage and wound healing (Wang et al. 2007; Nakano et al. 2008). While studying the interaction of ZO-1 with Cx43 gap junctions in HeLa cells, it was observed that Green Fluorescent Protein (GFP)

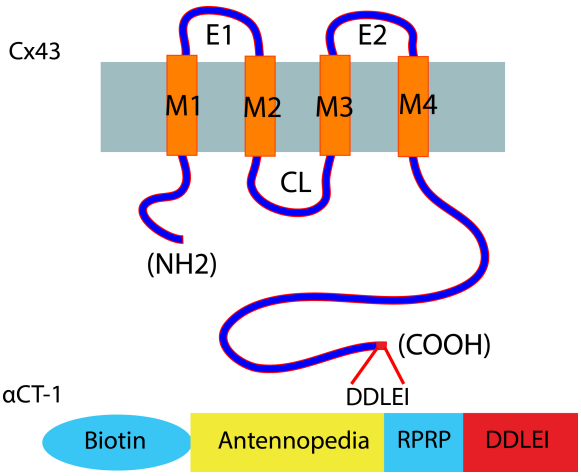

Figure 1.2: Structures of Cx43 protein and αCT-1 peptide (Hunter et al. 2005).

tagged Cx43CT resulted in an increase in the size of gap junctions by interfering with the ZO-1/Cx43 interaction. Upon introducing a synthetic peptide sequence (αCT-1) which mimics a portion of the Cx43CT, the the experiment was repeated yielding a similar outcome (Hunter et al. 2005). The αCT-1 peptide contains the last nine amino acids of Cx43CT, an antennopedia region to aid in cellular uptake, and biotin for easy detection. The peptide works by binding to the PDZ2 domain of ZO-1 which is where Cx43CT normally binds. It may also bind to the other proteins that bind to the Cx43CT or to the cytoplasmic loop of Cx43 (Rhett et al. 2008; Bouvier et al. 2009). αCT-1 has been shown to accelerate wound closure rates while also reducing scar tissue formation in cutaneous injuries in porcine models (Ghatnekar et al. 2009) as well as limiting gap junction remodeling and improving heart function following cryo-injury (O'Quinn et al. 2011). The peptide also increases PKCϵ related phosphorylation of Cx43CT-Ser368 after injury (Palatinus, Rhett, and Gourdie 2011).

1.4 Bone Marrow Stromal Cells

Bone marrow stromal cells (BMSCs; sometimes referred to as bone mesenchymal stem cells) were chosen as the tissue culture model for this study. BMSCs have been shown to be multipotent stem cells and can differentiate into numerous cell types

(Pittenger 1999; Jiang et al. 2002) and have been shown to have a significant role in wound healing (Bucala et al. 1994; Seppanen et al. 2013). They have also been shown to be easily transfected and capable of expressing proteins for extended periods (Hurwitz et al. 1997; Krebsbach et al. 2003; Aluigi et al. 2006).

1.5 Epithelial-Mesenchymal Transformation

Due to the widespread effects of αCT-1 on wound healing and the many protein interactions of Cx43CT, it has been hypothesized that a cell signaling pathway known as the Epithelial-Mesenchymal Transformation (EMT) may be involved in the mechanism of αCT-1. EMT is a group of pathways involved in the transformation of cells from an epithelial phenotype to a mesenchymal phenotype. In addition to a change in gene and protein expression, there is a decrease in cell to cell junctions, adoption of a spindle morphology, and increased migratory capabilities. EMT is classified into three types: type 1-embryogenesis and organ development, type 2-wound healing, and type 3-cancer growth and metastasis (Kalluri and Weinberg 2009). Type 2 EMT is necessary in wound healing as the cells adjacent to the wound need to move into the gaps left by the wound. Epithelial cells will undergo EMT, lose their polarity, dissociate from neighboring cells, and migrate into the wound area.

In preliminary studies in our lab, we used a PCR Super Array (Qiagen) with EMT genes to study how rat BMSCs reacted to αCT-1. These results, found in Appendix A, showed up-regulation of the genes for Keratin19 (Krt19), Matrix metalloproteinase-3 (Mmp3), F11r (Junctional Adhesion Molecule-A, JAM-A), and several others. These genes were chosen for further study in a more detailed experiment. In addition, Snai2 was chosen due to its role as a transcription factor involved in initializing EMT (Savagner, Yamada, and Thiery 1997; Bolos 2002), as well as Cx43 and ZO-1 due to their central role in the action of the peptide. *In vitro* scratch assays were performed on rat BMSCs to determine whether these genes are altered, and to show that the

EMT pathway is a possible mechanism for the increased healing caused by the αCT-1 peptide.

Chapter 2

Methods

2.1 Cell Isolation and Expansion

The following procedures were performed according to the animal experimentation guidelines set forth by the Institutional Animal Care and Use Committee (IACUC), of the University of South Carolina School of Medicine. Rat BMSCs were isolated from the bone marrow of rats (Sprague Dawley). The rats were sacrificed by dry ice asphyxiation. The femur and tibia were removed and cleaned of any remaining soft tissues. The interior of the bones were flushed with primary culture media (Dulbecco's Modified Eagle Medium supplemented with 5% fetal bovine serum, 50 μg/mL gentamicin, and 250 ng/mL amphotericin B) into 50 mL conical tube. The tube was centrifuged at 800 rpm for 8 minutes. After removing the supernatant, the cells were resuspended in primary culture media. The cells were placed in T75 flasks (Greiner), and placed in an incubator set at 5% CO_2 and 37°C for one week. Media was replaced as needed, usually after 1-2 weeks or when the cells had attached to the flask. Once the cells were at 90% confluency, they were passaged by rinsing with Moscona's solution (in mM: 136.8 NaCl, 28.6 KCl, 11.9 NaHCO3, 9.4 glucose, 0.08 NaH2PO4, pH 7.4), trypsinizing with 0.05% trypsin/0.1% EDTA and plating again in two T75 flasks. If necessary cells were frozen in liquid nitrogen. Cells to be used for analysis were thawed and then passaged and placed into 6-well plates (RNA analysis), 12-well plates (protein analysis), 6-well plates on coverslips (confocal microscopy), or MatTek dishes (live cell imaging).

2.2 Gene Expression Analysis

Scratch Assay

Once the cells had grown to become 90% confluent the scratch assay was performed. The media was removed from the wells, and the wells were rinsed with Moscona's Solution. Two parallel scratches, each 2cm long and 1cm apart, were made near the center of the well using a 20μL pipette tip (ART). The wells were rinsed once more with Moscona's Solution. Four time points were taken for both αCT-1 and control samples: an unscratched sample (time=0), one hour, two hour, and three hour.

A solution made of αCT-1 dissolved in Moscona's solution to a concentration of 100μM. 20μL of this solution was placed on each scratch of the test samples, and for the control samples 20μL of Moscona's solution was placed on the scratches. The dishes were placed in the incubator for 30 minutes then primary culture media was added to each well. The RNA was extracted immediately for the no scratch samples and at one, two, and three hours later for the other time points.

RNA Extraction

To extract the RNA, the wells were rinsed with Moscona's solution. Then, using a RNeasy Mini Kit (Qiagen), 350 mL of the RLT buffer and 5μL of β-mercaptoethanol were added to each well. The cells were agitated and mixed with the pipette tip. The solution was then transferred to a 1.5mL centrifuge tube and frozen at -20°C.

After thawing the RNA extract, the RNA lysate was transferred to a RNeasy spin column. The extraction was performed as described by the manufacturers instructions described as follows.

- Add 500μL of 70% ethanol to the RLT lysate and mix by pipetting
- Transfer solution to spin column and centrifuge for 15 seconds

- Add 700μL of Buffer RW1 to the spin column and spin for 15 seconds
- Add 500μL of Buffer RPE to the spin column and spin for 15 seconds
- Add 500μL of Buffer RPE to the spin column and spin for 2 minutes
- Add 25μL of RNase-free water to spin column and spin for 1 minutes and collect flow-through
- Repeat prior step to collect remainder of RNA

The collected RNA was frozen and stored at -20°C.

RNA Analysis & cDNA Synthesis

The RNA concentration and RNA Integrity Number (RIN) were obtained by using a mRNA Nano Chip and running it on the 2100 Bioanalyzer (Agilent). The results can be found in Appendix C. An iScript cDNA Kit (Bio-Rad) was used to transcribe cDNA from the RNA. For each sample, 1μg of RNA was added to a mixture of 8μL of iScript 5x Reaction mix, 2μL of Reverse Transcriptase, and RNase-Free water for a total volume of 80μL. The mixture was run in a iCycler Thermal Cycler (Bio-Rad) for 5 minutes at 25°C, 30 minutes at 42°C, 5 minutes at 85°C, and then stored at 4°C.

qPCR

In order to quantify the gene expression, qPCR was carried out using a CFX Connect (Bio-Rad, Hercules, CA). Primers (Integrated DNA Technologies) were designed using Primer BLAST (National Institute of Health). The primers were designed to have a melt temperature near 60$\pm$2°C. A two step protocol was used with an annealing temperature of 58°C and a melt temperature of 95°. A melt curve was used

Table 2.1: Primers used in qPCR

mRNA	Forward Primer	Reverse Primer	Product Size
ARBP	CGACCTGGAAGTCCAACTAC	ATCTGCTGCATCTGCTTG	109
Cx43	TCAGCCTCCAAGGAGTTCCACCAAC	GCACTGACAGCCACACCTTCCC	159
F11r	TGTTCCCAGCGGAGTTGCGG	CCGAACCCTTGCCTTGCACC	111
Krt19	GCACTGTGGCAGAGATAGAGG	TGAGCTGATACTCCTGGT	132
Mmp3	GGAGGCAGCAAAGAACCCGCT	GGGTAGGATGAGCACACAGCCG	111
Snai2	CCAGGCTAGGAAATCGTTCA	TGGGTGAACCTGGAAAGGTA	107
ZO-1	CCATCTTTGGACCGATTGCTG	TAATGCCCGAGCTCCGATG	123

starting at 70° to check for any primer dimers or multiple transcripts. Primer efficiencies were determined using serial dilutions of rat tongue cDNA. In each well, 6.25ng of cDNA (1μL) was loaded into 19μL of master-mix containing primers and SSoAdvanced SYBR Green Supermix (Bio-Rad, Hercules, CA). qBase+ (Bio-Gazelle) was used to process the data using the Pfaffl Method (Pfaffl 2001) by normalizing the target transcript relative quantities to acidic ribosomal phosphoprotein P0 (ARBP) relative quantities. Analysis of variance (ANOVA) was used to determine which transcripts were affected by the time and treatment. Bonferroni post testing was performed to compare time point pairs of each gene.

2.3 Protein Analysis

Scratch Assay

For the protein isolation, plated as described above except using 12-well plates in order to reduce biological noise from cells that were not near the scratch. Samples were agitated in the presence of 350μL of T-Per Buffer (Thermo Scientific) with the addition of 1% HALT Protease Inhibitor (Thermo Scientific). The protein samples were centrifuged and the supernatant was collected to remove any cellular debris. Samples from three wells were combined and concentrated using a 10 kDa Microcon Concentrator (Milipore) to increase the protein concentration by reducing the volume of the sample. A Bradford Coomassie Assay was performed to determine the concentration of each sample.

Western Blotting

Western blotting was performed on the treated and untreated cells in order to determine the effect of αCT-1 treatment resulting in any changes in the protein concentration of the EMT markers following injury. Bio-Rad Criterion Gels 4-15% with 12+2 45μL wells were used. For each sample, 20μg of protein was dissolved in 20μL of water, then mixed in a 1:1 ratio with Laemmli Buffer with 5% β-mercaptoethanol. The sample solutions were then denatured by heating in a water bath at 70°C for 10 minutes. The samples were then loaded into the gel alongside 20μL of Dual Color Precision Protein Standard (Bio-Rad). The gels were run at 125V for 1-1.5 hours, until the loading dye had almost reached the bottom of the gel. The protein was transferred to supported nitrocellulose membranes using a Criterion Blotter (Bio-Rad) at 100V for 45 minutes.

The blots were then rinsed with Phosphate Buffer Solution (PBS) with 0.05% Tween20 3 times for 5 minutes. The blots were blocked for an hour in 5% Blotting Grade Milk Blocker (Bio-Rad) dissolved in PBS. The blots were probed with the with primary antibodies in 1:1000 (except for 1:500 for Krt19) dilutions in 5% milk blocker in PBS-Tween overnight at 4°. After rinsing in PBS-Tween, the blots were probed with horseradish peroxidase conjugated secondary antibodies for 1 hour in the same dilution and buffer as the primary antibodies. The blots were then sprayed with HyGlo ECL (Denville Scientific) and agitated for 1 minute. Images of the blots were captured using an autoradiography cassette and HyGlo Film (Denville Scientific) with exposure times between 8 seconds and 3 minutes. Densitometry was performed using ImageJ (NIH) and ERK-1 as a normalizing protein.

Table 2.2: Antibodies used in western blotting and confocal microscopy

Protein	Host	Manufacturer	Catalog #	Size (kDa)
Erk-1	Mouse	BD	610030	42-44
Cx43	Mouse	Millipore	MAB3067	43
ZO-1	Mouse	Developmental Studies Hybridoma Bank	R26.4C	225
Krt19	Mouse	Novus	NBII 42238	40-44
Snai2	Rabbit	Santa Cruz	sc-15391	34
Mmp3	Rabbit	Santa Cruz	sc-6839-r	53
JAM-A	Rabbit	Santa Cruz	sc-25629	32
anti-Mouse HRP	Goat	Invitrogen	M30107	N/A
anti-Rabbit HRP	Goat	Invitrogen	656120	N/A
anti-Mouse 546	Goat	Life Technologies	A-11035	N/A
anti-Rabbit 546	Goat	Life Technologies	A-11030	N/A

2.4 Confocal Microscopy

Scratch Assay

In order to determine the cellular localization of the various proteins following scratch and treatment, confocal micrscopy was performed. The cells were grown on coverslips placed in 6-well plates. The cells were rinsed with Moscona's Solution then scratched. The scratches were made in a direction so that the most confluent cells would be subjected to the scratch. Each coverslip was scratched twice using a P20 pipette tip. The cells were rinsed again, then the peptide or control solutions were added to each scratch. After incubating for 30 minutes, the cells were rinsed again, then media was added. At each time point, the cells were rinsed and then fixed using 2% paraformaldehyde in PBS for 10 minutes. The cells were then rinsed in 0.01M Glycine in PBS twice for 15 minutes before being permeabilized with 0.1% Triton X-100/0.01M Glycine/PBS.

Fluorescence Antibody Staining

The coverslips were rinsed between each of the following steps by rinsing in PBS for five minutes three times, except after the initial blocking step. The coverslips were blocked in 5% Bovine Serum Albumin in PBS for one hour. They were then probed with the primary antibodies in 5% BSA/PBS (1:200) for one hour. They were

then stained with Alexa Fluor 546 IgG(H+L) highly cross adsorbed (Life Technologies) secondary antibodies in 5%BSA/PBS (1:250) for one hour. Next, F-Actin was stained with Alexa Fluor 488 Phalloidin (Life Technologies) in PBS (1:200). Finally, the nuclei were stained with 4',6-Diamidino-2-Phenylindole (DAPI) (1:2500). The coverslips were mounted on slides using 1,4-diazabicyclo[2.2.2]octane (DABCO).

Confocal Microscopy Imaging

The images were captured using a Zeiss LSM 510 microscope. The lasers used were the 405nm, Argon 488nm, and HeNe 543nm. All images were taken using a 63X oil immersion objective. Multi-track image collection was used in order to prevent cross-talk between channels by imaging one channel at a time with filters to block non-specific emissions. Emission from some fluorophores can excite fluorophores of longer wavelengths leading to some channels showing fluorescence from another fluorophore.

2.5 Live Cell Imaging

Scratch Assay

Cells were grown in 35mm MatTek Dishes (MatTek) until they were 90% confluent. After being rinsed with Moscona's Solution, cells were scratched then rinsed again. Cells were only scratched once since the microscope is not equipped with a automated stage and thus can only image one area per frame. 100 μL of 100μM αCT-1 dissolved in primary culture media was added to the dish and allowed to incubate for 30 minutes. Then 1 mL of media was added to the dish to sustain the cells during imaging.

Image Acquisition

Images were acquired using a Zeiss Axiovert 200M Inverted Microscope. A 10X phase contrast objective was used in combination with a HAL 100 light source. The

microscope chamber was set 37°C and 5% CO_2 and allowed to preheat for several hours to prevent focal drift. Images were collected every 6 minutes over 24 hours using AxioVision software.

Image Analysis

In order to measure migration, several MATLAB functions were written to automate this process and can be found in Appendix D. Each image was subtracted from next image in the time series, to remove any static objects and leave only portions where cells moved. A Wiener filter was used to remove additional noise from the subtracted images. The filtered image was thresholded to a black and white image. Any objects near the top of the image were removed to avoid measure cells from the opposite side of the scratch. A dilation morphological filter was used to fill in some of the smaller gaps left over. Objects smaller than 5000 pixels were removed from the image to remove random debris from detection. Then, using the regionprops function, total area of all of the objects on the screen was measured.

Chapter 3

Results

3.1 Gene Expression

Previous in vivo studies have shown that the αCT-1 renders an effect on cells within 2 hours of application (Ghatnekar et al. 2009). Time points at 1, 2, and 3 hours were chosen in order to study the effect on mRNA transcripts around the 2 hour window. For each time point there were three samples taken from different culture wells. Analysis of the qPCR data shows that the time from scratch and treatment with αCT-1 changed the expression of several genes. Cx43 expression showed no difference between control and αCT-1 samples, but both samples showed equal reduction in expression with time. In contrast, expression of F11r increased over time in both samples peaking at 2 hours, but αCT-1 samples were consistently greater with significant increases at 2 and 3 hours. Krt19 followed a similar pattern of increasing expression with time, and significant increases in the αCT-1 samples at 2 and 3 hours. Mmp3 showed little variation with the exception of the two hour time point during which the αCT-1 sample showed a significant decrease before increasing back above the control levels. Snai2 failed to show any significant differences between αCT-1 and control, but showed a steady decrease with time in both samples. Finally, ZO-1 remained stable throughout the 3 hour time period with only minor fluctuations.

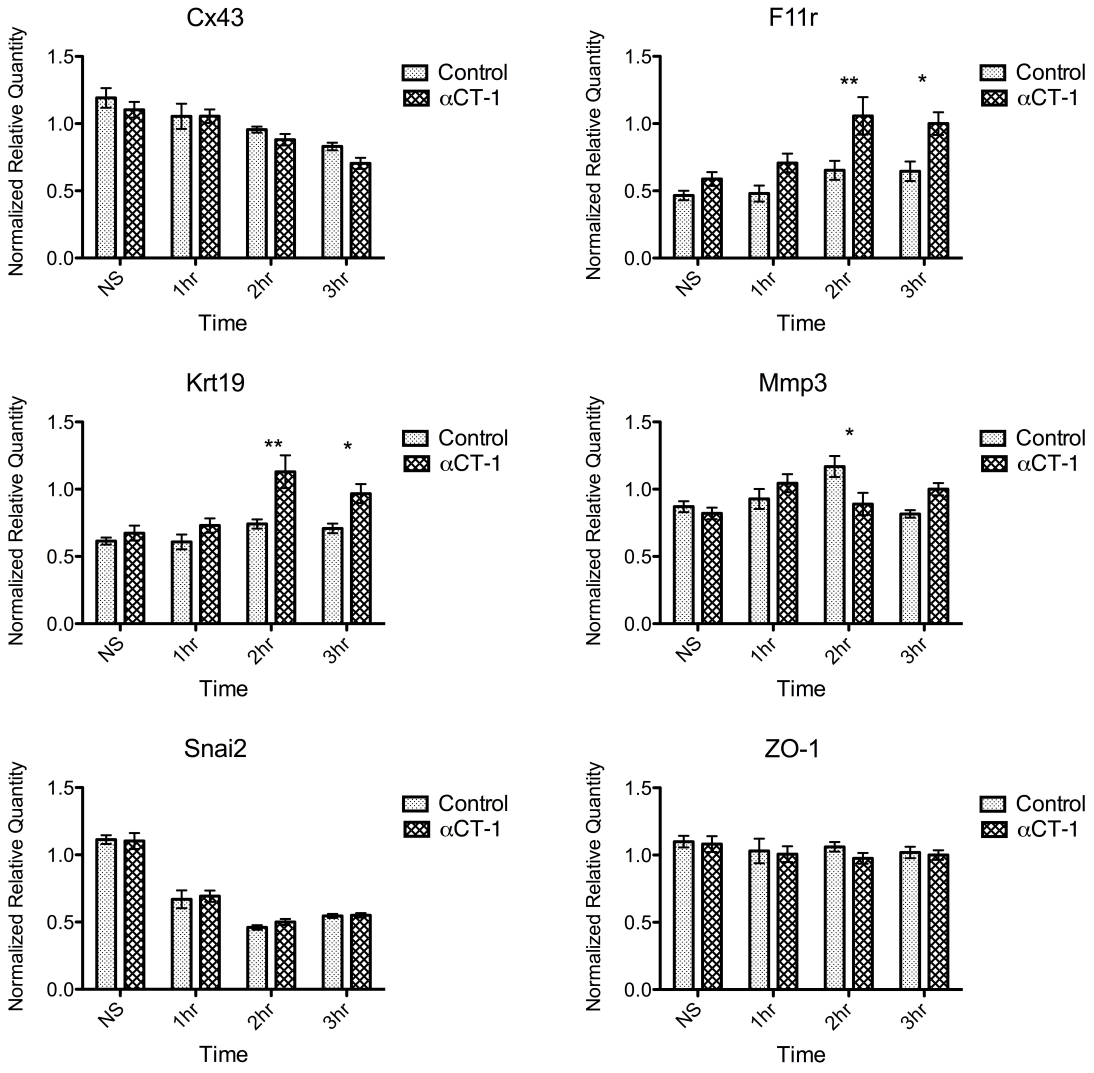

Figure 3.1: Results of qPCR analysis showing effects of αCT-1 on gene expression. Bars represent standard error. Single asterisks indicate $p<0.05$, double asterisks indicate $p<0.01$ (n=3).

Table 3.1: ANOVA of qPCR Results

Gene	Time	Treatment
Cx43	*<0.001	0.082
F11r	*0.001	*<0.001
Krt19	*<0.001	*<0.001
Mmp3	0.354	0.873
Snai2	*<0.001	0.629
ZO-1	0.424	0.346

Table of p-values for the ANOVA performed qPCR expression values. P-value<0.05 is considered significant and indicated with an asterisk.

3.2 Protein Expression

In order to determine whether the changes in gene expression carried over into protein expression, western blotting was performed at the same time points. Due to various problems with protein extraction and antibodies, only one blot was imaged for each protein. Extracellular-signal-regulated kinase 1 (ERK-1) is stably expressed and was used to determine normalization factors for densitometry as shown in Appendix B. It showed consistent bands confirming that it was not affected by the peptide. For Cx43, αCT-1 treated samples showed higher expression in the no scratch and one hour samples, yet lower expression in the two and three hour samples. Cx43 showed two distinct bands, possibly the P0 and P1/P2 states, but due to the wide range of proteins being analyzed the gel resolution for such close bands was minimal. The results for Krt19 were similar to the gene expression results as the αCT-1 samples were greater for all points except the three hour sample. Yet the protein analysis of JAM-A (corresponding to gene F11r), showed little relation with control samples showing higher expression the no scratch and three hour samples, no difference at one hour, and a slight increase in αCT-1 at two hours. Likewise, Mmp3 control samples showed higher expression in the no scratch and 1 hour sample which inverted in the two and three hour samples with the three hour control showing almost no expression.

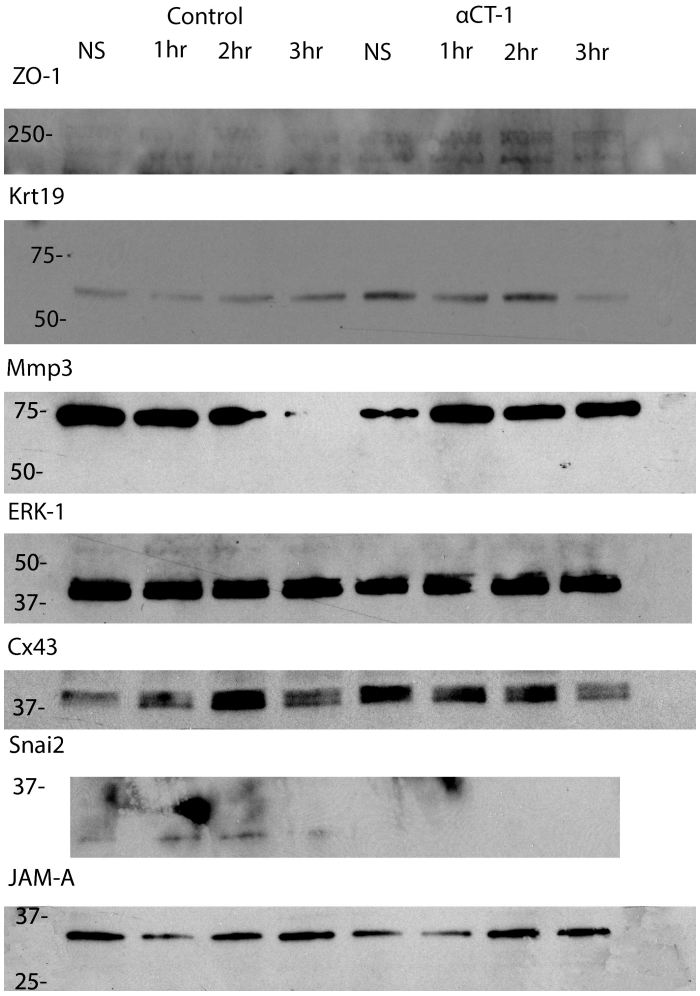

Figure 3.2: Images of western blots for each protein.

Snai2 had the most noticeable results with a complete absence of protein in all of the αCT-1 samples. Finally, ZO-1 showed slight increase in αCT-1 in the no scratch and three hour sample, with no difference at one hour, and a large increase at 2 hours.

It should be noted that western blotting often lacks the sensitivity required to discern the small changes in protein expression that may occur in this experiment without running numerous replicates The faint bands for ZO-1 can be attributed to larger proteins being more difficult to transfer. Many of the bands showed minimal changes between samples. Despite having faint bands, Snai2 is the only protein that was completely down-regulated due to the αCT-1 treatment.

3.3 Confocal Analysis

Confocal microscopy for Cx43 showed increased gap junction size as mentioned in Hunter et al. 2005. The location of Cx43 within the cells showed no pattern or orientation relative to the scratch border. Few gap junctions are visible in the images and are sporadic. JAM-A appeared in small amounts throughout the cells. It typically appeared in small clusters, but it was difficult to discern any consistent localization results. However, Krt19 yielded no information as it appeared to be equally dispersed throughout the cells in all samples. Images for Mmp3 showed differences in localization between control and αCT-1 treated cells. Control samples showed protein scattered throughout the cells evenly, yet in the αCT-1 samples the protein localized to the nucleus and the area surrounding the nucleus. Snai2 tended to aggregate in and near the nucleus, but this localization was repeated across all samples. ZO-1 also showed a lack of information; it appeared spread throughout the cell equally.

Looking at the the F-actin staining, it appeared that the αCT-1 had an effect on the structure of actin. The F-actin filaments in the αCT-1 cells appear to be thinner and more linear compared to the disperse and overlapping structure of the untreated cells. Also, in the αCT-1 samples the actin filaments appear to not attach to the cell membrane compared to the control samples. These changes appear to be greatest two hours after the scratch.

3.4 Cell Migration

To investigate the effect of αCT-1 on cell migration and movement, live cell imaging was used to image the cells with a temporal resolution of 6 minutes over 24 hours. Cell migration showed clear differences between the control samples and the peptide treated samples. Looking at the total area occupied by cells in the image, the control

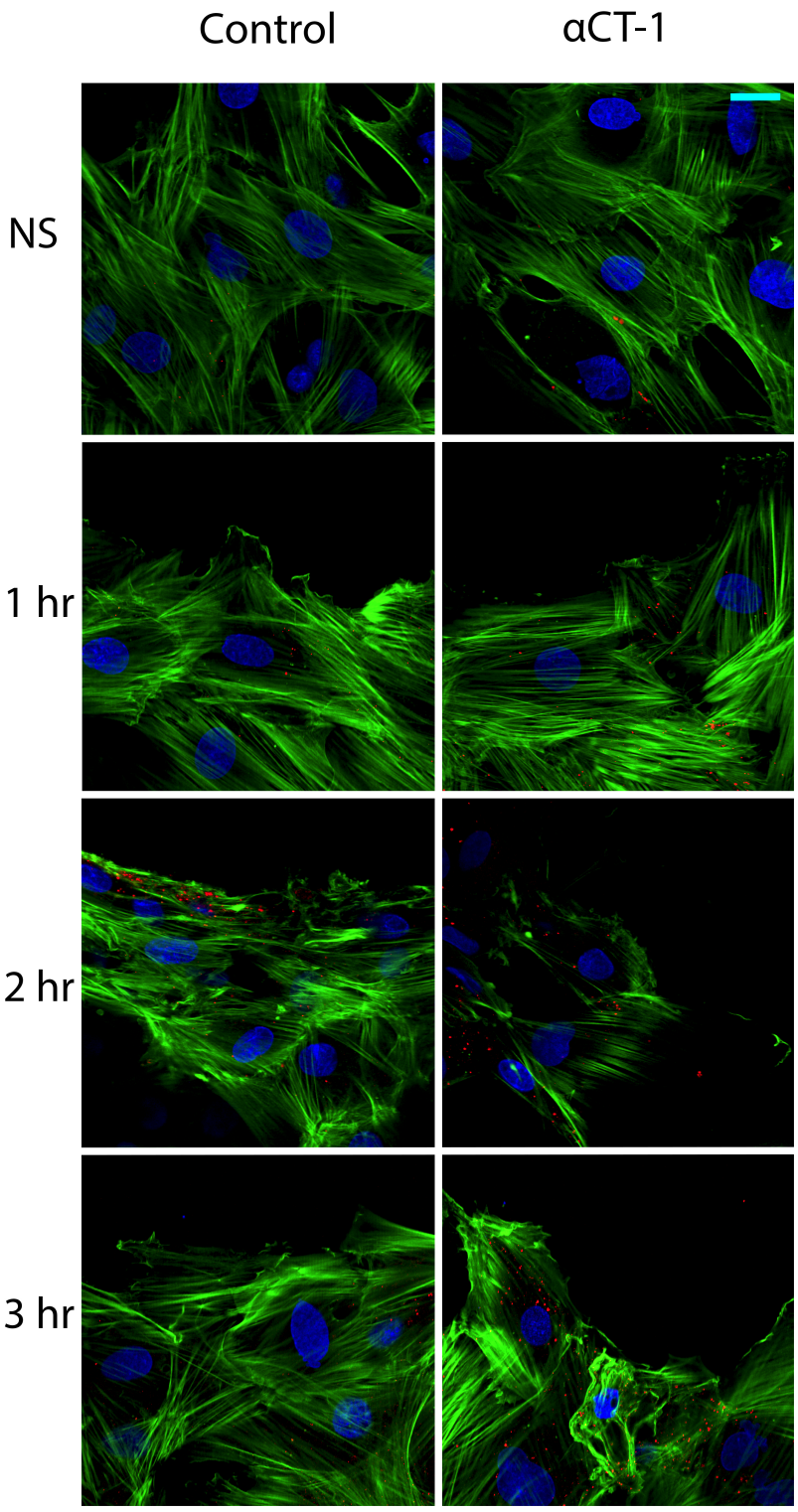

Figure 3.3: Confocal microscopy images of Cx43 stained cells. Blue-nucleus (DAPI), Green-F-Actin (Phalloidin), Red-Cx43 (Cy-3). Scratches are located on the top border of each image except for the no scratch (NS) samples. Smaller gap junctions plaques can be seen in the αCT-1 treated samples. Scale bar=20μm.

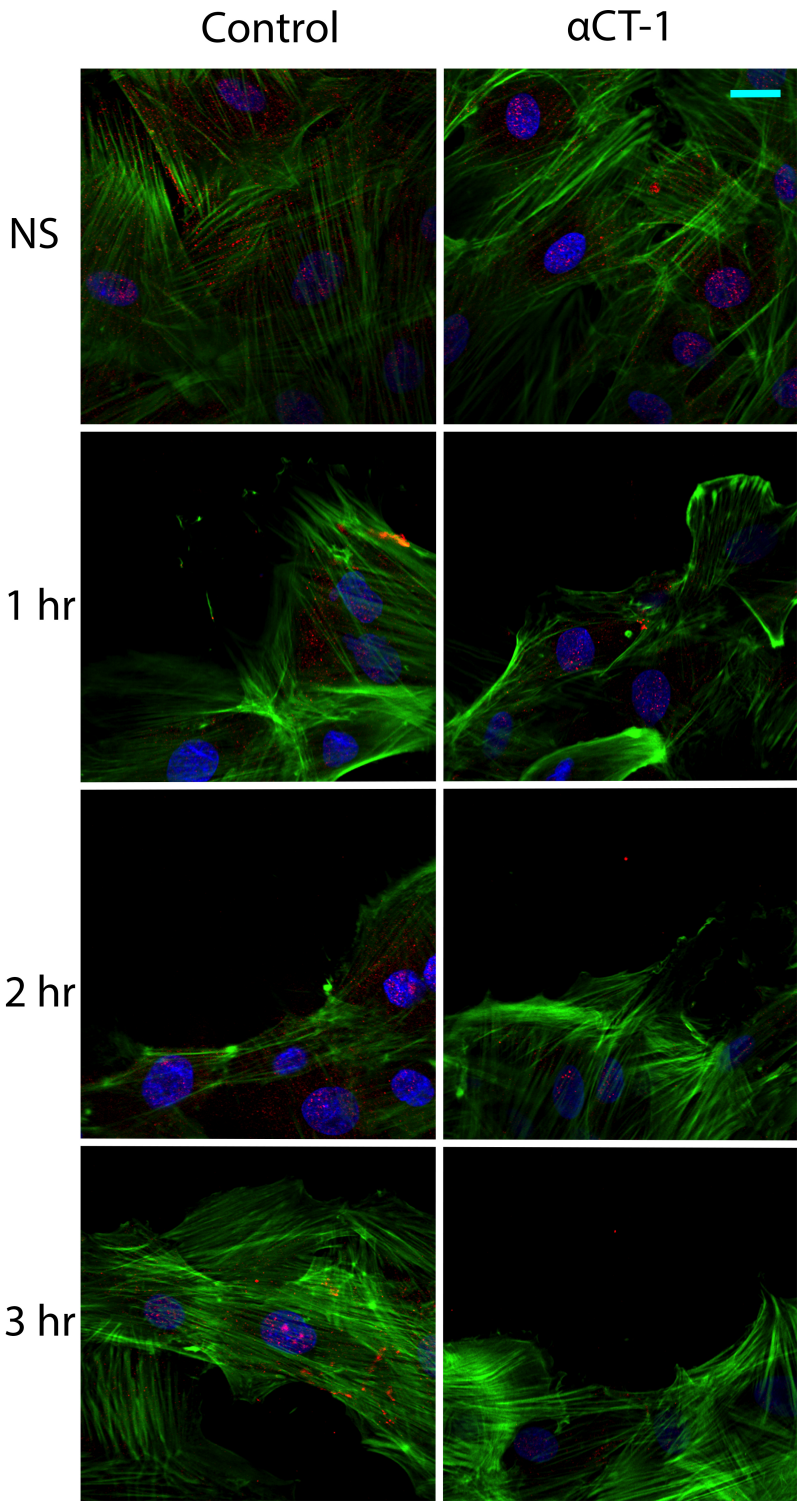

Figure 3.4: Confocal microscopy images of Mmp3 stained cells. Blue-nucleus (DAPI), Green-F-Actin (Phalloidin), Red-Mmp3 (Cy-3). Scratches located on the top border of each image except for the no scratch (NS) samples. Scale bar=20μm.

.

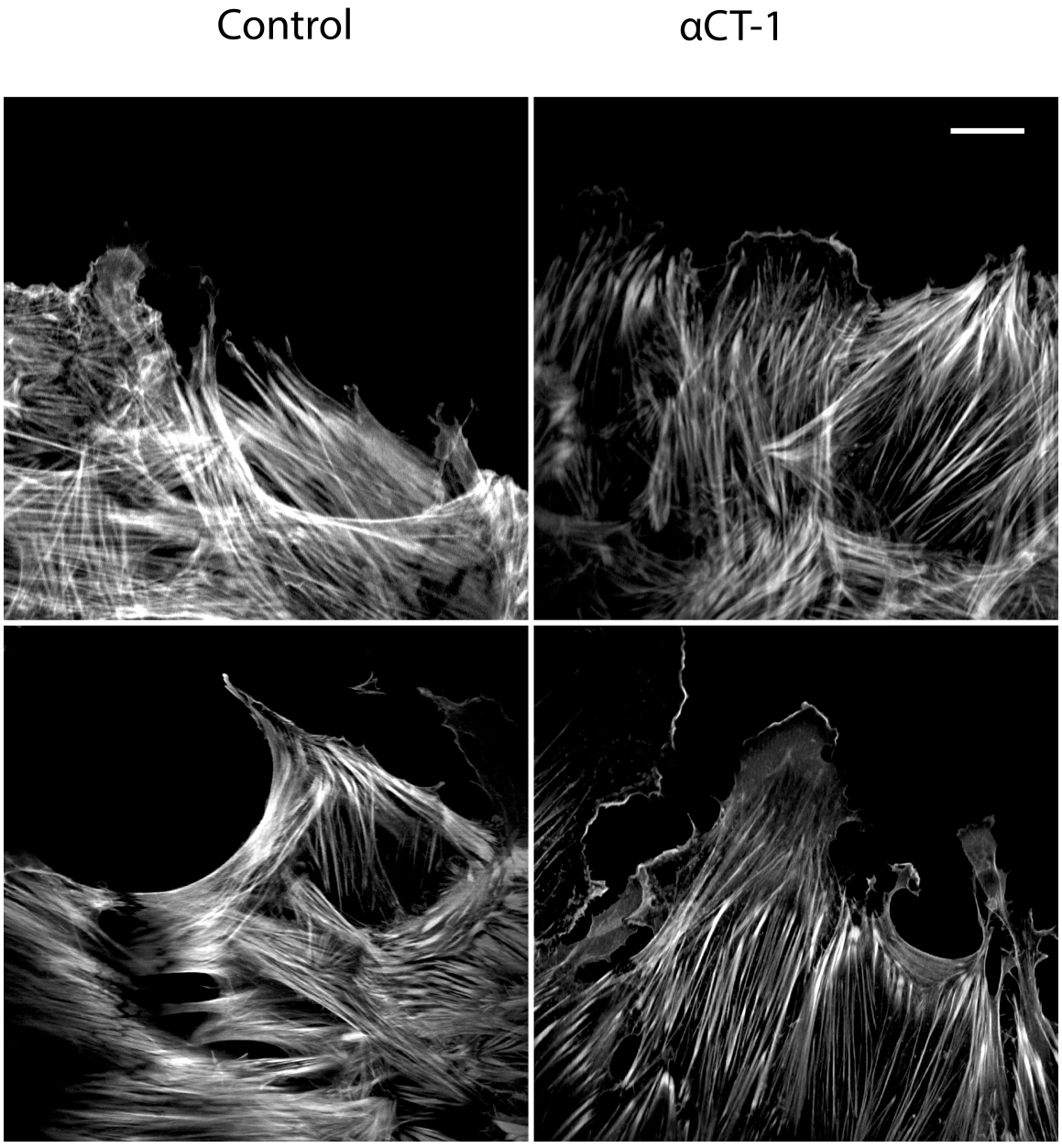

Figure 3.5: Confocal microscopy images of just actin in two hour samples. Scale bar=20μm.

samples filled in more of the scratch void than the peptide samples. As shown in Figure 3.7, all samples start moving at roughly the same rate, yet at around 7 hours the peptide treated cells slow down and cease advancing. This is also shown in the images in Figure 3.6. The αCT-1 treated cells begin to separate from each other and begin to ruffle their edges while not moving, seemingly losing all directionality of movement. The cells on the edge of the scratch void move forwards at first, but the cells behind them do not follow leading to large gaps between cells. In contrast, the control cells maintain their cell-cell contacts and move together as a monolayer. Cells at the front of the scratch edge maintain coordinated migration towards the scratch void, and cells behind the leading edge continue to move behind the leading cells preventing large gaps from forming. The control cells also showed large lamellipodia with some cells reach across others to enter the scratch void. These were completely absent in the αCT-1 treated cells, as they only showed shorter protrusions that did not lead to cell movement.

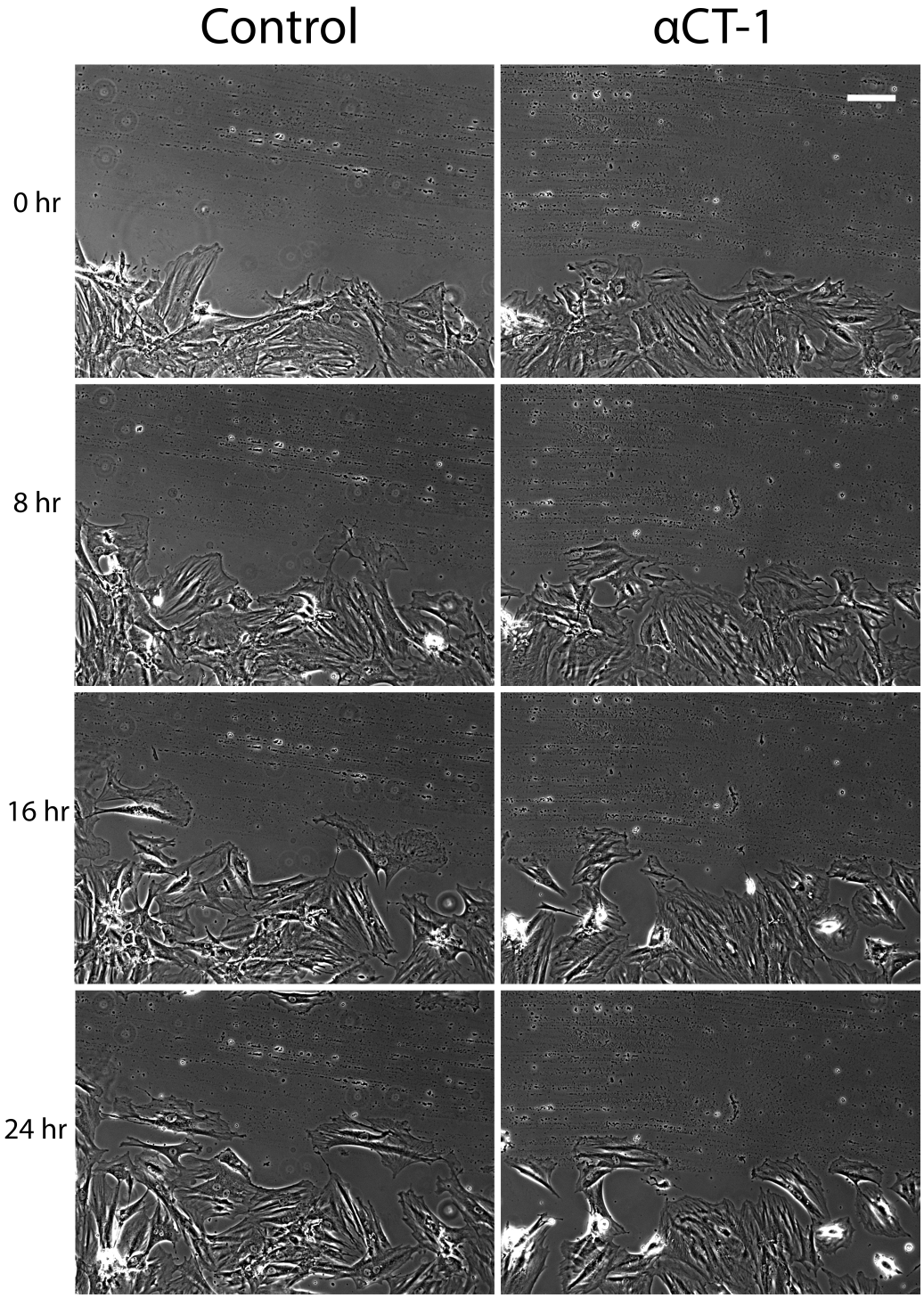

Figure 3.6: Images showing control and peptide treated cells migrating across the scratch void at time intervals of 8 hours over a 24 hour period. Scale bar=100μm

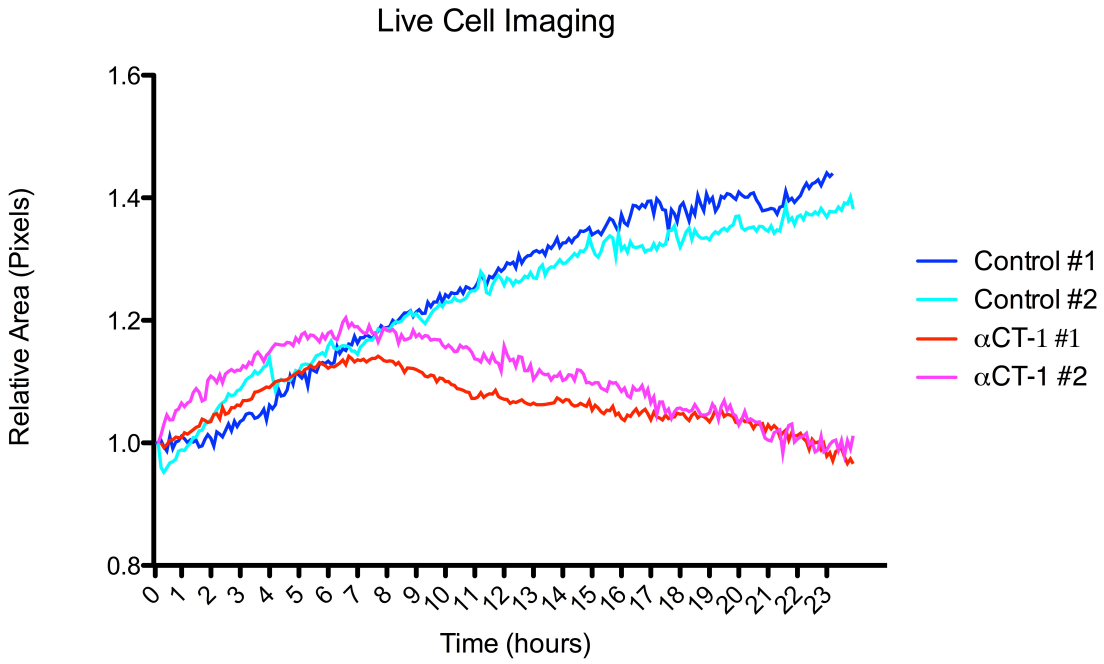

Figure 3.7: Cell migration analysis showing the relative area, normalized against initial area, of cells migrating across scratch over a 24 hour period.

Chapter 4

Discussion

Previous work done has demonstrated the healing properties of αCT-1 but has focused on the tissue level effects (Ghatnekar et al. 2009; Soder et al. 2009) or the Cx43/ZO-1 interaction (Hunter et al. 2005; Hunter and Gourdie 2008). Due to these wound healing effects, it is likely that the extent of the mechanism of αCT-1 extends beyond its effects on Cx43 and ZO-1. In order to identify other possible changes induced by αCT-1, the EMT pathway was chosen due to its role in wound healing.

In EMT, proteins related to tight junctions (JAM-A) and the cytoskeleton (Krt19) are normally down-regulated to allow for cell migration. Looking at just the gene expression of the no scratch samples, Krt19 is increased with αCT-1 treatment and Mmp3 is decreased. At the two hour time point, there was the greatest number of significant changes in gene expression with F11r, Krt19, and Mmp3 all showing significance. Snai2 has been shown to be an effective transcriptional factor for inducing the EMT pathway (Savagner, Yamada, and Thiery 1997; Bolos 2002). Snai2 showed a steady decline in gene expression with time, yet this was not matched by western blot analysis. There was a complete absence of Snai2 protein in the αCT-1 samples, differing from the expected up-regulation normally shown in EMT. Mmp3 is normally up-regulated in EMT to break down the extracellular matrix. Confocal microscopy showed more evenly distributed Mmp3 in the control samples compared to the αCT-1 samples, and the western blotting showed similar results in protein quantity. The western blot and confocal microscopy results for Mmp3 may not be

accurate since it is a secreted protein. Zymography would have to be carried out to measure extracellular Mmp3 levels.

The live cell imaging results showed every characteristic expected of EMT: cells adopting spindle morphologies, accelerated movement, and the breakdown of cell-cell contacts. The cessation of movement at around seven hours is unusual as the cells continue to ruffle the membranes, but they lack any orientation in their movements. There are two possible explanations for this lack of movement. First, the cells may still be capable of moving but are unable to either control the direction of movement or can no longer detect the driving signal of movement. Second, the cells are not migration towards anything, but instead are moving away from other cells. It appears that once cells on the leading edge move enough to lose contact, they cease to move.

The changes in F-actin may also support EMT. During the process of EMT, the actin structures have been shown to be remodeled as they lose connections to membrane proteins and must make connections elsewhere (Yilmaz and Christofori 2009). This event may stem from αCT-1 disrupting the ZO-1/Cx43 interaction. ZO-1 acts a scaffold between the membrane proteins and actin by providing binding areas for both proteins (González-Mariscal, Betanzos, and Avila-Flores 2000; Rhett, Jourdan, and Gourdie 2011). The removal of ZO-1 from gap junctions may reduce the available binding locations for actin to connect with the membrane. This may explain the decreased structure and spindle morphology shown in the treated samples in live cell imaging. With the decreased actin structure, the cell may be forced to adopt a more morphology requiring less support.

The data suggests that there are two opposing activities occurring within the cells; the gene and protein expression indicating no relation to EMT, but the movement and structure of the cell indicate EMT has occurred. There are several possibilities for these mixed results. The EMT pathway contains numerous different genes and proteins. It is possible that the genes chosen in this study are not part of the EMT

pathway triggered by αCT-1. These cells are also already mesenchymal cells. The EMT pathways can achieve little overall change to these cells; the only change to be expected would be a shift from stationary mesenchymal cells to more mobile and invasive cells.

Research on αCT-1 has so far only shown the effects on wound healing, Cx43, and gap junctions. The down regulation of Cx43 with time that occurs between treated and untreated samples is to be expected as it has been shown that Cx43 expression is reduced following injury (Mori et al. 2006). Yet this change in expression does not match with the protein results, albeit possibly due to limited sample size for the western blot analysis. The confocal images of Cx43 show the expected increase in gap junction size, but this alone does not seem to be enough to explain the change in the cell movement. Due to the peptide acting on the PDZ2 of ZO-1, the effect on the cell can stretch well beyond altering gap junction activity. The effect seen with JAM-A may be caused by the altered ZO-1. JAM-A has been shown to bind to the PDZ3 of ZO-1 and aid in the formation of adherens-like junctions (Morris et al. 2006). ZO-1 also has a homologous protein, ZO-2, that can bind to the PDZ2 domain to aid in the formation of scaffolding structure attached to tight junctions (Fanning et al. 1998; Itoh et al. 1999). The PDZ2 domain has also shown to be necessary for the proper formation of bands of tight junctions located at the perimeter of epithelial cells (Rodgers et al. 2012).

The interference in the normal activity of ZO-1 may explain the changes in gene expression. The αCT-1 peptide alone may be enough to induce morphological and migratory changes that occur in EMT, yet EMT is normally induced by growth factors or other factors altering transcription directly. The gene and protein expression seen may have been a result in a reaction to this EMT-like behavior. The cell may try to restore itself back to its normal state by reducing EMT related gene expression, which would explain the lack of Snai2 protein, up-regulation of Krt19 and JAM-A,

and down-regulation of Mmp3. With the altered activity of ZO-1 the changes in expression may not materialize due to changes in protein interactions.

Chapter 5

Conclusion

This study shows that EMT may not be an affected pathway of rat BMSCs when treated with αCT-1, yet it demonstrates the extent of its effects on gene expression and cell movement. These effects go well beyond the immediate changes caused by the Cx43/ZO-1 interaction. Further research will be required to understand how Cx43 and ZO-1 can effect these studied genes and proteins.

The genes in this study were limited to the EMT pathway, but there may be other genes affected by αCT-1. With the recent discovery of new protein interactions with the Cx43CT such as Akt (Park et al. 2009), CCN3 (Fu et al. 2004), v-Src (Lin et al. 2001), c-Src (Sorgen et al. 2004b), and P2Y1 (Scemes 2008), it is necessary to determine if any of these proteins may be disrupted by αCT-1 either through blocking interactions or direct binding. One approach for discovering the affected proteins, is to continue work on immunoprecipitation assays similar to those previously done in Hunter et al. 2005. It is also important to look at the role that the Cx43CT has on DNA synthesis (Doble et al. 2004) and cell proliferation (Dang, Doble, and Kardami 2003).

Further research will be necessary to determine the full extent of effects that αCT-1 has on BMSCs and even other cell types. Epithelial cell types should be similarly tested as they may show a more significant change along the EMT pathway. In addition, wound model studies can be performed to study delivery of the peptide. BMSCs have been shown to improve healing when implanted into damaged tissue as well as being capable of expressing transfected genes and naturally assisting in wound

healing (Hurwitz et al. 1997; Studeny et al. 2002; Aluigi et al. 2006; Shen et al. 2006; Rong et al. 2008). Due to the short time of effect of the peptide, this could serve as a way of extending the release for longer periods of time. Studying the combined effect on an *in vivo* animal model using this method may prove to be a promising long term treatment to accelerate wound healing and reduce scar tissue. There are many possible uses and applications of the peptide, and with further understanding of the its mechanism of action, it may prove to be a powerful tool in the treatment of injury and disease.

Bibliography

Akoyev, Vladimer and Dolores J. Takemoto (2007). "ZO-1 is required for Protein Kinase C Gamma-driven Disassembly of Connexin43". *Cell Signaling* 19.5, pp. 958–967.

Alexander, David B and Gary S Goldberg (Oct. 2003). "Transfer of biologically important molecules between cells through gap junction channels." *Current Medicinal Chemistry* 10.19, pp. 2045–58.

Aluigi, Michela et al. (Feb. 2006). "Nucleofection is an efficient nonviral transfection technique for human bone marrow-derived mesenchymal stem cells." *Stem Cells* 24.2, pp. 454–61.

Bao, Xiaoyong, Luis Reuss, and Guillermo a Altenberg (May 2004). "Regulation of purified and reconstituted connexin 43 hemichannels by protein kinase C-mediated phosphorylation of Serine 368." *The Journal of Biological Chemistry* 279.19, pp. 20058–66.

Beyer, Eric C, David L Paul, and Daniel A Goodenough (Dec. 1987). "Connexin43: a protein from rat heart homologous to a gap junction protein from liver." *The Journal of Cell Biology* 105.6 Pt 1, pp. 2621–9.

Bolos, V. (Dec. 2002). "The transcription factor Slug represses E-cadherin expression and induces epithelial to mesenchymal transitions: a comparison with Snail and E47 repressors". *Journal of Cell Science* 116.3, pp. 499–511.

Bouvier, Denis et al. (Dec. 2009). "Characterization of the structure and intermolecular interactions between the connexin40 and connexin43 carboxyl-terminal and cytoplasmic loop domains." *The Journal of Biological Chemistry* 284.49, pp. 34257–71.

Bucala, R et al. (Nov. 1994). "Circulating fibrocytes define a new leukocyte subpopulation that mediates tissue repair." *Molecular Medicine* 1.1, pp. 71–81.

Dang, Xitong, Bradley W Doble, and Elissavet Kardami (Jan. 2003). "The carboxy-tail of connexin-43 localizes to the nucleus and inhibits cell growth." *Molecular and cellular biochemistry* 242.1-2, pp. 35–8.

Doble, Bradley W et al. (Jan. 2004). "Phosphorylation of serine 262 in the gap junction protein connexin-43 regulates DNA synthesis in cell-cell contact forming cardiomyocytes." *Journal of Cell Science* 117.Pt 3, pp. 507–14.

Duffy, Heather S et al. (Sept. 2002). "pH-dependent intramolecular binding and structure involving Cx43 cytoplasmic domains." *The Journal of Biological Chemistry* 277.39, pp. 36706–14.

Ek-Vitorin, Jose F et al. (June 2006). "Selectivity of connexin 43 channels is regulated through protein kinase C-dependent phosphorylation." *Circulation Research* 98.12, pp. 1498–505.

Fanning, Alan S, Thomas Y Ma, and James Melvin Anderson (Nov. 2002). "Isolation and functional characterization of the actin binding region in the tight junction protein ZO-1." *FASEB Journal: Official Publication of the Federation of American Societies for Experimental Biology* 16.13, pp. 1835–7.

Fanning, Alan S et al. (1998). "The Tight Junction Protein ZO-1 Establishes a Link between the Transmembrane Protein Occludin and the Actin Cytoskeleton". *The Journal of Biological Chemistry* 273.45, pp. 29745–29753.

Friend, Daniel S and Norton B Gilula (1972). "Variations in tight and gap junctions in mammalian tissues". *Journal of Cell Biology* 53, pp. 758–776.

Fu, Christine T et al. (Aug. 2004). "CCN3 (NOV) interacts with connexin43 in C6 glioma cells: possible mechanism of connexin-mediated growth suppression." *The Journal of Biological Chemistry* 279.35, pp. 36943–50.

Ghatnekar, Gautam S et al. (2009). "Connexin43 carboxyl-terminal peptides reduce scar progenitor and promote regenerative healing following skin wounding". *Regenerative Medicine* 4.2, pp. 205–223.

Giepmans, Ben N G (May 2004). "Gap junctions and connexin-interacting proteins." *Cardiovascular Research* 62.2, pp. 233–45.

Giepmans, Ben N G and W H Moolenaar (1998). "The gap junction protein connexin43 interacts with the second PDZ domain of the zona occludens-1 protein." *Current Biology* 8.16, pp. 931–934.

González-Mariscal, L, A Betanzos, and A Avila-Flores (Aug. 2000). "MAGUK proteins: structure and role in the tight junction." *Seminars in Cell & Developmental Biology* 11.4, pp. 315–24.

Goodenough, Daniel A and David L Paul (July 2009). "Gap junctions." *Cold Spring Harbor Perspectives in Biology* 1, a002576.

He, D S et al. (May 1999). "Formation of heteromeric gap junction channels by connexins 40 and 43 in vascular smooth muscle cells." *Proceedings of the National Academy of Sciences of the United States of America* 96.11, pp. 6495–500.

Hunter, Andrew W and Robert G Gourdie (May 2008). "The second PDZ domain of zonula occludens-1 is dispensable for targeting to connexin 43 gap junctions." *Cell Communication & Adhesion* 15.1, pp. 55–63.

Hunter, Andrew W et al. (2005). "Zonula Occludens-1 Alters Connexin43 Gap Junction Size and Organization by Influencing Channel Accretion". *Molecular Biology of the Cell* 16.December, pp. 5686–5698.

Hurwitz, David R et al. (1997). "Systemic Delivery of Human Growth Hormone or Human Factor IX in Dogs by Reintroduced Genetically Modified Autologous Bone Marrow Stromal Cells". *Human Gene Therapy* 156, pp. 137–156.

Itoh, Masahiko et al. (1999). "Direct Binding of Three Tight Junction-associated MAGUKs, ZO-1, ZO-2, and ZO-3, with the COOH Termini of Claudins". *The Journal of Cell Biology* 147.6, pp. 1351–1363.

Jiang, Yuehua et al. (2002). "Pluripotency of mesenchymal stem cells derived from adult marrow". *Nature* 418, pp. 41–49.

Kalluri, Raghu and Robert A Weinberg (2009). "The basics of epithelial-mesenchymal transition". *The Journal of Clinical Investigation* 119.6, pp. 1420–1428.

Krebsbach, Paul H et al. (Jan. 2003). "Bone marrow stromal cells as a genetic platform for systemic delivery of therapeutic proteins in vivo: human factor IX model." *The Journal of Gene Medicine* 5.1, pp. 11–7.

Kumar, Nalin M and Norton B Gilula (1996). "The Gap Junction Communication Channel". *Cell* 84, pp. 381–388.

Lin, J H et al. (Oct. 1998). "Gap-junction-mediated propagation and amplification of cell injury." *Nature Neuroscience* 1.6, pp. 494–500.

Lin, R et al. (Jan. 2001). "v-Src-mediated phosphorylation of connexin43 on tyrosine disrupts gap junctional communication in mammalian cells." *Cell Communication & Adhesion* 8.4-6, pp. 265–9.

Milks, L C et al. (Oct. 1988). "Topology of the 32-kd liver gap junction protein determined by site-directed antibody localizations." *The EMBO Journal* 7.10, pp. 2967–75.

Moreno, a. P. (Jan. 2002). "Role of the Carboxyl Terminal of Connexin43 in Transjunctional Fast Voltage Gating". *Circulation Research* 90.4, pp. 450–457.

Mori, Ryoichi et al. (Dec. 2006). "Acute downregulation of connexin43 at wound sites leads to a reduced inflammatory response, enhanced keratinocyte proliferation and wound fibroblast migration." *Journal of Cell Science* 119.Pt 24, pp. 5193–203.

Morris, Andrew P et al. (2006). "Junctional Adhesion Molecules (JAMs) are differentially expressed in fibroblasts and co-localize with ZO-1 to adherens-like junctions." *Cell Communication & Adhesion* 13.4, pp. 233–47.

Musil, L S and D a Goodenough (Sept. 1993). "Multisubunit assembly of an integral plasma membrane channel protein, gap junction connexin43, occurs after exit from the ER." *Cell* 74.6, pp. 1065–77.

Nakano, Yukiko et al. (Jan. 2008). "Connexin43 knockdown accelerates wound healing but inhibits mesenchymal transition after corneal endothelial injury in vivo." *Investigative Ophthalmology & Visual Science* 49.1, pp. 93–104.

O'Quinn, Michael P et al. (2011). "A Peptide Mimetic of the Connexin43 Carboxyl Terminus Reduces Gap Junction Remodeling and Induced Arrhythmia Following Ventricular Injury". *Circulation Research* 108, pp. 704–715.

Palatinus, Joseph a, J Matthew Rhett, and Robert G Gourdie (Aug. 2012). "The connexin43 carboxyl terminus and cardiac gap junction organization." *Biochimica et Biophysica Acta* 1818.8, pp. 1831–43.

Palatinus, Joseph a., Joshua M. Rhett, and Robert G. Gourdie (May 2011). "Enhanced PKCϵ mediated phosphorylation of connexin43 at serine 368 by a carboxyl-terminal mimetic peptide is dependent on injury". *Channels* 5.3, pp. 236–240.

Park, Darren J et al. (2009). "Akt Phosphorylates Connexin43 on Ser373, a "Mode-1" Binding Site for 14-3-3". *Cell Communication & Adhesion* 14.5, pp. 211–226.

Perkins, G a, Daniel A Goodenough, and G E Sosinsky (Mar. 1998). "Formation of the gap junction intercellular channel requires a 30 degree rotation for interdigitating two apposing connexons." *Journal of Molecular Biology* 277.2, pp. 171–7.

Peters, N. S. et al. (Sept. 1993). "Reduced content of connexin43 gap junctions in ventricular myocardium from hypertrophied and ischemic human hearts". *Circulation* 88.3, pp. 864–875.

Pfaffl, MW (2001). "A new mathematical model for relative quantification in real-time RT-PCR". *Nucleic Acids Research* 29.9, pp. 16–21.

Pittenger, M. F. (Apr. 1999). "Multilineage Potential of Adult Human Mesenchymal Stem Cells". *Science* 284.5411, pp. 143–147.

Reaume, AG et al. (1995). "Cardiac malformation in neonatal mice lacking connexin43". *Science* 267, pp. 1831–4.

Rhett, J Matthew, Jane Jourdan, and Robert G Gourdie (May 2011). "Connexin 43 connexon to gap junction transition is regulated by zonula occludens-1." *Molecular Biology of the Cell* 22.9, pp. 1516–28.

Rhett, J Matthew et al. (Apr. 2008). "Novel therapies for scar reduction and regenerative healing of skin wounds." *Trends in Biotechnology* 26.4, pp. 173–80.

Rodgers, Laurel S et al. (2012). "Epithelial barrier assembly requires coordinated activity of multiple domains of the tight junction protein ZO-1." *Journal of Cell Science* February 2013.

Rong, Shu-ling et al. (2008). "Effects of transplanted myoblasts transfected with human growth hormone gene on improvement of ventricular function of rats". *Chinese Medical Journal* 121.30470457, pp. 347–354.

Ruiz, Mariana (2006). URL: `http://en.wikipedia.org/wiki/File:Connexon_and_connexin_structure.svg#file`.

Savagner, P, K M Yamada, and J P Thiery (June 1997). "The zinc-finger protein slug causes desmosome dissociation, an initial and necessary step for growth factor-induced epithelial-mesenchymal transition." *The Journal of Cell Biology* 137.6, pp. 1403–19.

Scemes, Eliana (2008). "Modulation of astrocyte P2Y1 receptors by the carboxyl terminal domain of the gap junction protein Cx43". *GLIA* 56, pp. 145–153.

Segretain, Dominique and Matthias M Falk (Mar. 2004). "Regulation of connexin biosynthesis, assembly, gap junction formation, and removal." *Biochimica et Biophysica Acta* 1662.1-2, pp. 3–21.

Seppanen, Elke et al. (Jan. 2013). "Distant mesenchymal progenitors contribute to skin wound healing and produce collagen: evidence from a murine fetal microchimerism model." *PloS One* 8.5, e62662.

Shen, L H et al. (Jan. 2006). "Intracarotid transplantation of bone marrow stromal cells increases axon-myelin remodeling after stroke." *Neuroscience* 137.2, pp. 393–9.

Soder, Brent L et al. (May 2009). "The connexin43 carboxyl-terminal peptide ACT1 modulates the biological response to silicone implants." *Plastic and Reconstructive Surgery* 123.5, pp. 1440–51.

Solan, Joell L and Paul D Lampe (Apr. 2009). "Connexin43 phosphorylation: structural changes and biological effects." *The Biochemical Journal* 419.2, pp. 261–72.

Solan, Joell L et al. (Dec. 2007). "Phosphorylation at S365 is a gatekeeper event that changes the structure of Cx43 and prevents down-regulation by PKC." *The Journal of Cell Biology* 179.6, pp. 1301–9.

Sorgen, Paul L et al. (July 2004a). "pH-dependent dimerization of the carboxyl terminal domain of Cx43." *Biophysical Journal* 87.1, pp. 574–581.

Sorgen, Paul L et al. (Dec. 2004b). "Structural changes in the carboxyl terminus of the gap junction protein connexin43 indicates signaling between binding domains for c-Src and zonula occludens-1." *The Journal of Biological Chemistry* 279.52, pp. 54695–701.

Stergiopoulos, K. et al. (May 1999). "Hetero-Domain Interactions as a Mechanism for the Regulation of Connexin Channels". *Circulation Research* 84.10, pp. 1144–1155.

Studeny, Matus et al. (July 2002). "Bone marrow-derived mesenchymal stem cells as vehicles for interferon-beta delivery into tumors." *Cancer research* 62.13, pp. 3603–8.

Toyofuku, Toshihiko et al. (1998). "Direct Association of the Gap Junction Protein Connexin-43 with ZO-1 in Cardiac Myocytes". *Journal of Biological Chemistry* 273.21, pp. 12725–12731.

Unger, Vinzenz M et al. (Feb. 1999). "Three-dimensional structure of a recombinant gap junction membrane channel." *Science* 283.5405, pp. 1176–80.

Wang, Chiuhui Mary et al. (2007). "Abnormal Connexin Expression Underlies Delayed Wound Healing in Diabetic Skin". *Diabetes* 56.November, pp. 2809–2817.

Wu, Jiahn-Chun, Ru-Yin Tsai, and Tun-Hui Chung (Mar. 2003). "Role of catenins in the development of gap junctions in rat cardiomyocytes." *Journal of Cellular Biochemistry* 88.4, pp. 823–35.

Yilmaz, Mahmut and Gerhard Christofori (June 2009). "EMT, the cytoskeleton, and cancer cell invasion." *Cancer Metastasis Reviews* 28.1-2, pp. 15–33.

Appendix A

EMT PCR Super Array Results

Table A.1: Genes in EMT Array

Ahnak	Col5a2	Fgfr2	Ilk	Mmp2	Ptk2	Sox10	Tgfb3	Wnt5a
Akt1	Ctgf	Fkbp1a	Itga5	Mmp3	Ptp4a1	Sparc	Timp1	Wnt5b
Bmp7	Ctnnb1	Fn1	Itgav	Mmp9	Rac1	Spp1	Tmeff1	Zeb1
Cald1	Dsc2	Foxc2	Itgb1	Msn	Rgs2	Stat3	Tmem132a	Zeb2
Camk2n1	Dsp	Fzd7	Jag1	Nodal	Serpine1	Steap1	Tspan13	Rplp1
Cav2	Egfr	Gng11	Krt14	Notch1	Sip1	Tcf3	Twist1	Hprt1
Cdh1	Erbb3	Gsc	Krt19	Ocln	Smad2	Tcf4	Vcan	Rpl13a
Cdh2	Esr1	Gsk3b	Krt7	Pdgfrb	Snai1	Tfpi2	Vim	Ldha
Col1a2	F11r	Igfbp4	Map1b	Plek2	Snai2	Tgfb1	Vps13a	Actb
Col3a1	Fgfbp1	Il1rn	Mitf	Ppp3r1	Snai3	Tgfb2	Wnt11	

Table A.2: EMT Array Trial 1

Up-regulated		Down-regulated	
Gene	Fold Change	Gene	Fold Change
Jag1	2.0028	Nodal	-2.3102
Tgfb2	2.1765	Il1rn	-2.5456
Mmp3	2.2377		
Dsp	2.7359		
Krt14	2.9938		
Esr1	3.2989		
F11r	4.0897		
Krt19	15.9115		

Table A.3: EMT Array Trial 2

Up-regulated		Down-regulated	
Gene	Fold Change	Gene	Fold Change
Sox10	2.1258	None	-
Krt19	19.4002		

Appendix B

Protein Densitometry

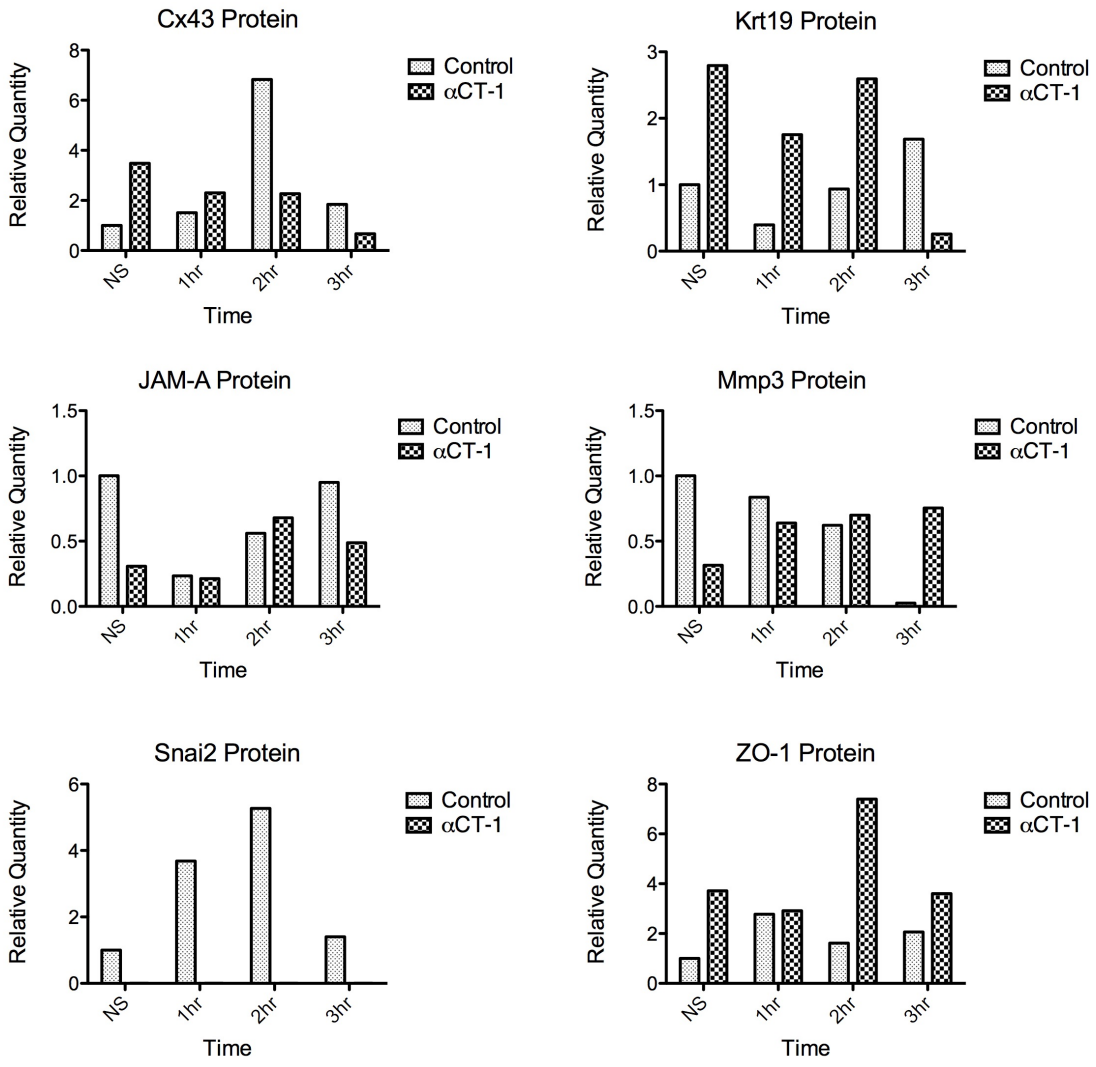

Figure B.1: Densitometry analysis of all proteins normalized against ERK-1. n=1.

Appendix C

Bioanalyzer Results

Table C.1: RNA concentration and RIN

Treatment	Time	Sample	RIN	Concentration (ng/μL)
Control	NS	1	9.5	48
Control	NS	2	9.6	51
Control	NS	3	9.6	54
Control	1 hr	1	9.5	55
Control	1 hr	2	9.7	60
Control	1 hr	3	9.5	52
Control	2 hr	1	9.3	76
Control	2 hr	2	9.6	70
Control	2 hr	3	9.5	59
Control	3 hr	1	9.5	76
Control	3 hr	2	9.6	67
Control	3 hr	3	9.8	64
αCT-1	NS	1	9.8	41
αCT-1	NS	2	9.7	42
αCT-1	NS	3	9.6	37
αCT-1	1 hr	1	9.6	50
αCT-1	1 hr	2	9.6	37
αCT-1	1 hr	3	9.7	34
αCT-1	2 hr	1	9.9	65
αCT-1	2 hr	2	9.5	44
αCT-1	2 hr	3	9.8	36
αCT-1	3 hr	1	9.8	42
αCT-1	3 hr	2	9.9	42
αCT-1	3 hr	3	9.6	33

Appendix D

MATLAB Image Processing Code

D.1 Function: importimages

```
1 function [importedimages, width, height, ImagesImported,
    FileTif]=importimages(skipimage)
2 %% Import Images
3
4 FileTif=uigetfile('*.tif');
5 InfoImage=imfinfo(FileTif);
6 width=InfoImage(1).Width;
7 height=InfoImage(1).Height;
8 NumberImages=length(InfoImage);
9 counter=0;
10 if skipimage==0
11     importedimages=zeros(height,width,NumberImages,'uint8');
12     tic
13     x=0;
14     for i=1:NumberImages
15         x=x+1;
16         importedimages(:,:,x)=imread(FileTif,'Index',i);
17     end
18     t=toc;
```

```
19      ImagesImported=x;
20      t;
21 else
22      importedimages=zeros(height,width,NumberImages/skipimage
            +1,'uint8');
23      tic
24      x=0;
25      for i=1:skipimage:NumberImages
26          x=x+1;
27          importedimages(:,:,x)=imread(FileTif,'Index',i);
28      end
29      ImagesImported=x;
30      t=toc;
31      t;
32 end
33 end
```

D.2 Function: areameasure

```
1 function [outputimage, data, area, movieframe]=areameasure;
2
3 input=importimages(0);
4
5 %below values can be adjusted based on image
6 verticallimit=250;
7 smallobjectsize=5000;
8 threshold=3.75;
9 disk1=2;
```

```
10 disk2=5;
11
12 %start of analysis
13 [height, width, frames]=size(input);
14 data=zeros(1,4);
15 st=strel('disk',disk1);
16 st2=strel('disk',disk2);
17 Area=zeros(239);
18 Centroid=zeros(239,2);
19 overlayimage=zeros(height, width, 3, frames);
20 for ii=1:(frames-1)
21     diff=imabsdiff(input(:,:,ii),input(:,:,ii+1));
22     diffreduced=wiener2(diff);
23     bwimage=diffreduced>threshold;
24     dilate=imdilate(bwimage,st);
25     openimage=bwareaopen(dilate,smallobjectsize);
26     outputimage(:,:,ii)=imdilate(openimage,st2);
27     for kk=1:verticallimit
28         outputimage(kk,:,ii)=0;
29     end
30     bwdata=logical(outputimage(:,:,ii));
31     regiondata=regionprops(bwdata, 'Area', 'Centroid');
32     [structsize, blank]=size(regiondata);
33     area(ii,1)=0;
34     for jj=1:structsize
35         [spot, blank2]=size(data);
36         temparea=regiondata(jj,1).Area;
```

```
37            data(spot+1, 1)=regiondata(jj,1).Area;
38            data(spot+1, 2)=regiondata(jj,1).Centroid(1,1);
39            data(spot+1, 3)=regiondata(jj,1).Centroid(1,2);
40            data(spot+1, 4)=ii;
41            area(ii,1)=area(ii,1)+temparea;
42        end
43        boundary=bwperim(outputimage(:,:,ii),8);
44        overlayimagetemp=imoverlay(input(:,:,ii),boundary,[0 1
              0]);
45        movieframe(ii)=im2frame(overlayimagetemp);
46    end
47    end
```

D.3 Function: writemovie

```
1  function writemovie(moviedata, filename)
2
3  writerObj=VideoWriter(filename);
4  writerObj.FrameRate=10;
5  open(writerObj);
6  for ii=1:239
7      writeVideo(writerObj, moviedata(ii));
8  end
9  close(writerObj);
10 end
```